PNAS RESEARCH ARTICLE | BIOCHEMISTRY

Identification of FBLL1 as a neuron-specific RNA 2′-O-methyltransferase mediating neuronal differentiation

Deyu Zhang[a], Bo Li[a], Henan Xu[a], Jingying Li[b], Chao Ma[c], Wei Ge[b], Congcong Lu[a,1], and Xuetao Cao[a,b,1]

Edited by Chuan He, The University of Chicago, Chicago, IL; received April 6, 2024; accepted October 28, 2024 by Editorial Board Member James L. Manley

2′-O-methylation is one of the most prevalent RNA modifications found in different RNA types. However, the identities of enzymes participating in the transfer of methyl groups are not well defined. To date, fibrillarin (FBL) is the only known small nucleolar ribonucleoprotein (snoRNP) 2′-O-methyltransferase. Whether other snoRNP 2′-O-methyltransferases exist and their functions in targeting RNAs to determine cell differentiation and function need to be elucidated. Here, we identify FBL-like protein 1 (FBLL1) as a 2′-O-methyltransferase and find its function in promoting neuronal differentiation. We show that FBLL1 is a key snoRNP complex enzyme that transfers methyl groups to substrate RNAs both in vitro and in vivo. Moreover, FBLL1 exhibits different 2′-O-methyltransferase site selectivity from FBL and tissue-specific distribution. FBLL1 is preferentially expressed in the brain, especially in human neuron cells, and promotes neuronal differentiation through 2′-O-methylation of *GAP43* messenger RNA (mRNA). Knockdown of FBLL1, but not FBL, reduced 2′-O-methylation levels in GAP43 mRNA, decreased expression of GAP43 proteins, and eventually repressed neuronal differentiation. Our finding of neuron-specific FBLL1 adds insights into RNA modification in neurobiology and provides clues for understanding 2′-O-methylation in health and disease.

RNA modification | RNA methyltransferase | 2′-O-methylation | fibrillarin like protein 1 | neuronal differentiation

Significance

RNA modifications, such as 2′-O-methylation (Nm), have recently emerged as critical posttranscriptional regulators in cell fate and diseases. In this study, we uncover fibrillarin-like protein 1 (FBLL1) as a neuron-specific 2′-O-methyltransferase. Compared with the previously known FBL, FBLL1 shows a similar catalytic mechanism but different Nm site preferences and distinct functions for neuronal differentiation. Our study of neuron-specific FBLL1 broadens current knowledge about small nucleolar ribonucleoprotein (snoRNP)-dependent ribose methylation and adds insights into Nm in neurobiology and related diseases.

RNA modifications are critical in determining cell differentiation and functions and are involved in various physiological and pathological processes (1–4). They are changes to the chemical composition of RNA molecules posttranscriptional. To date, >150 different RNA modifications have been identified, including the most extensively investigated N6-methyladenosine (m6A). The mechanism of RNA modifications in posttranscriptional regulation is complex because of the involvement of multiple RNA-binding protein (RBP) activities, including writers, erasers, and readers (5–7). RNA modifications have recently emerged as critical posttranscriptional regulators of gene expression during lineage fate decisions in normal organ development and homeostasis (7, 8). For example, m6A is markedly increased during brain development and exhibits tissue-specific regulation (4, 9). Accumulating studies have linked dysregulation of RNA modifications to various diseases, including cancer, infection, autoimmune diseases, and neurological disorders (2, 8, 10). Unraveling the basic molecular functions of RNA modifications and identifying proteins responsible for writing, erasing, or regulating RNA modifications would deepen our understanding of life and provide targets for intervention in human diseases (11, 12).

2′-O-methylation (Nm, where N stands for any nucleotide) is one of the most pervasive RNA modifications in both noncoding and coding RNAs in almost all species (13, 14). Recent data revealed that Nm also occurs in low-abundance RNAs, such as messenger RNAs (mRNAs) and other small nuclear RNAs (15–17). Nm nucleotides are demonstrated to be associated with RNA stability (18) and also play a role in more subtle functions such as gene translation (19); they are even implicated in immune evasion mechanisms (20). However, the significance of various Nm sites is still poorly understood, and how Nm sites contribute to gene regulation and mRNA translation remains to be determined (13).

Despite decades of considerable effort, the identities of Nm-related RBPs are not well defined, limiting further understanding of the precise biological roles and functions of Nm. Unlike m6A and other methylation types (21, 22), no protein for removing Nm has been discovered. The formation of 2′-O-methylated residues is effected via two mechanisms: either stand-alone enzymes or box C/D small nucleolar RNA (snoRNA)-guided ribonucleoprotein (RNP) complexes (23, 24). Several stand-alone 2′-O-methyltransferases have recently been identified, broadening knowledge about snoRNA-independent ribose methylation. For instance, FTSJ3 was identified as a 2′-O-methyltransferase of HIV recruited through TRBP (TAR RNA-binding protein) to avoid innate immune sensing (25).

Author affiliations: [a]State Key Laboratory of Medicinal Chemical Biology, Institute of Immunology, College of Life Sciences, Nankai University, Tianjin 300071, China; [b]Department of Immunology, Center for Immunotherapy, Institute of Basic Medical Sciences, Peking Union Medical College, Chinese Academy of Medical Sciences, Beijing 100005, China; and [c]National Human Brain Bank for Development and Function, Chinese Academy of Medical Sciences, Beijing 100005, China

Author contributions: C.L. and X.C. designed research; D.Z., B.L., H.X., J.L., C.M., W.G., and C.L. performed research; D.Z., B.L., H.X., J.L., C.M., W.G., and C.L. analyzed data; and D.Z., W.G., C.L., and X.C. wrote the paper.

The authors declare no competing interest.

This article is a PNAS Direct Submission. C.H. is a guest editor invited by the Editorial Board.

[1]To whom correspondence may be addressed. Email: lucongcong@nankai.edu.cn or caoxt@immunol.org.

This article contains supporting information online at https://www.pnas.org/lookup/suppl/doi:10.1073/pnas.2406961121/-/DCSupplemental.

Published November 21, 2024.

Meanwhile, fibrillarin (FBL) is the only reported 2′-O-methyltransferase in a box C/D snoRNA-guided protein complex (23). Considering the importance and extensive distribution of Nm, and the well-known protein complexes for m6A modification, other small nucleolar RNP (snoRNP)-dependent enzymes for Nm may exist; this needs to be explored.

In this study, we identified FBL-like protein 1 (FBLL1) as a Nm transferase by mass spectrometry (MS). After forming a snoRNP complex with a box C/D snoRNA and other core proteins, FBLL1 transfers a methyl group to the 2′-hydroxyl of the ribose moiety in substrate RNAs both in vitro and in cells. Compared with FBL, FBLL1 exhibits different substrate site specificity and expression levels in different tissues and therefore different biological functions. Our results reveal that FBLL1 is enriched in neuron cells, and it can promote neuronal differentiation through increased GAP43 protein expression by mediating *GAP43* mRNA Nm modification.

Results

FBLL1 Is a Potential 2′-O-methyltransferase Preferentially Located in the Brain. Although it is one of the most widespread RNA modifications, the variation of the extent of Nm in distinct tissues remains unknown. To help understand the functions and regulatory mechanisms of Nm, we first quantified the relative abundance of Nm modifications in different tissues using a high-throughput liquid chromatography–MS (LC–MS) approach. Total RNAs were extracted from the brain, liver, lung, kidney, and spleen of the mouse (Strain: C57 BL6/J), respectively. After digestion into individual nucleosides, samples were separated by reverse-phase LC and analyzed by high-resolution MS. The relative abundances of Nm on all four nucleotides (Am, Gm, Cm, and Um) were measured (Fig. 1*A* and *SI Appendix*, Fig. S1 *A*–*C*). We noticed that Am was particularly abundant in the brain.

Over 85% of total RNA is ribosomal RNA (rRNA). In eukaryotic rRNA, Nm is carried out by box C/D snoRNP (26). Given the role of FBL as the only known snoRNP-dependent 2′-O-methyltransferase, we then examined the expression levels of FBL in distinct tissues. No enrichment of FBL in the brain relative to other tissues was observed at either the mRNA or protein levels (Fig. 1 *B* and *C*). Interestingly, a second band below the expected FBL band appeared in the brain samples in western blots (WB) using anti-FBL antibody. Using immunoprecipitation–MS, we determined that the protein in the lower band might be FBLL1 (Fig. 1*D*), and the presence of FBLL1 was further confirmed by WB by using anti-FBLL1 antibody (*SI Appendix*, Fig. S1*D*).

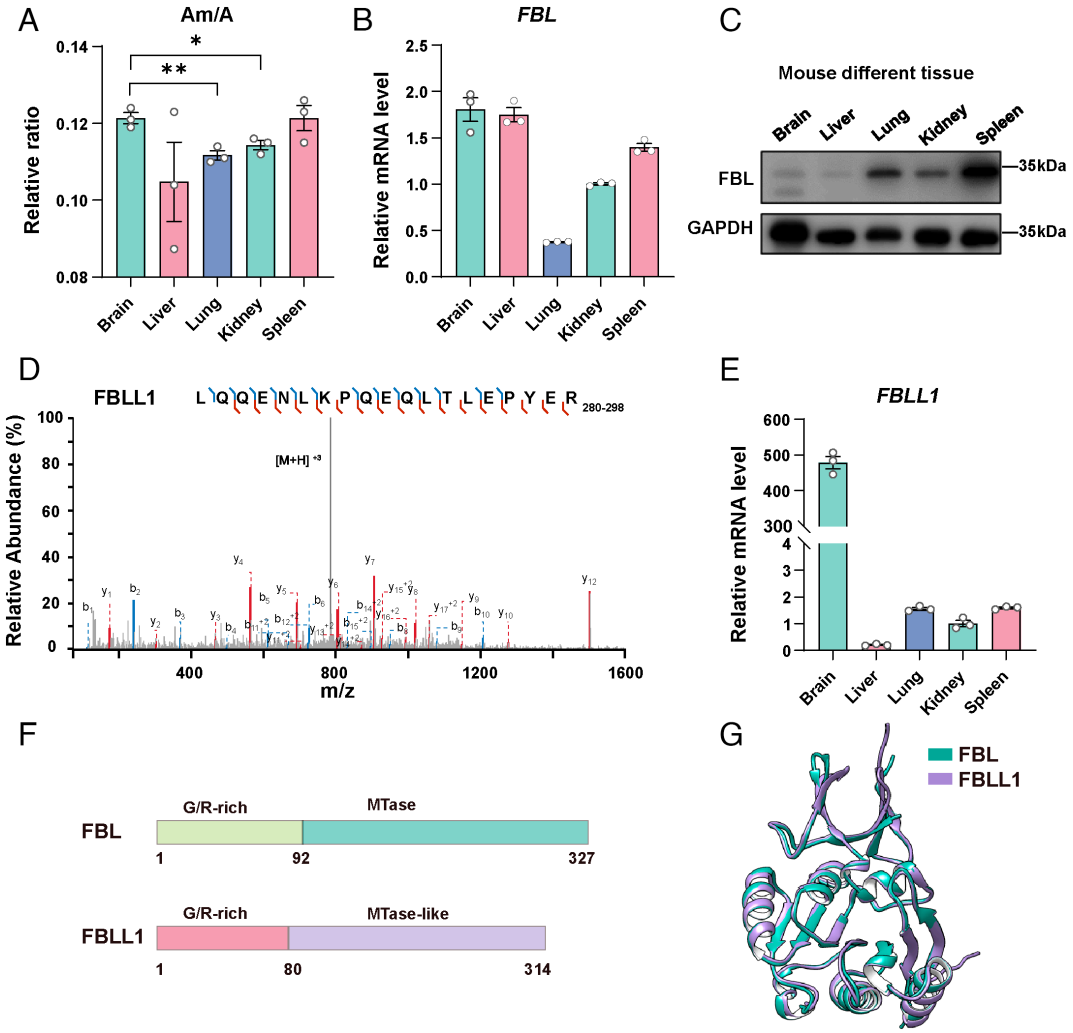

Fig. 1. FBLL1 is a potential 2′-O-methyltransferase located in the brain. (*A*) 2′-O-methylation levels of adenosine(A) in total RNA of mouse different tissues were quantified by LC–MS. (*B*) *FBL* mRNA level in mouse different tissues. (*C*) Western blot of FBL in mouse different tissues. (*D*) Tandem mass spectrum of the unique FBLL1 peptide LQQENLKPQEDLTLEPYER. The *y*- and *b*- series indicate fragments at amide bonds of the peptide. (*E*) FBLL1 mRNA level in mouse different tissues. (*F*) Domain architecture and sequence motif of mouse FBL and FBLL1. (*G*) Catalytic domain structure of human FBLL1 compared with human FBL (FBL, PDB: 7SE6; the structure of FBLL1 was predicted by AlphaFold2). Error bars, mean ± SEM; n = 3 (*A*, *B*, and *D*) biologically independent samples. *$P < 0.05$ and **$P < 0.01$.

RT-qPCR showed that *FBLL1* was highly expressed in brain compared with other tissues (Fig. 1*E*).

Like FBL, FBLL1 contains two domains, an *N*-terminal glycine-arginine-rich (G/R-rich) domain and a methyltransferase (MTase) domain at the *C* terminus (Fig. 1*F* and *SI Appendix*, Fig. S2). Studies have shown that the G/R-rich domain in FBL can be considered an evolutionary innovation in eukaryotes (23). It is highly disordered and variable between FBLL1 and FBL. Meanwhile, the MTase domain, which participates in the transfer of methyl groups, is extremely well-conserved throughout evolution. We compared the MTase domain structure of FBLL1 predicted by using AlphaFold2 with the FBL structure in the Protein Data Bank (PDB ID: 7SE6) and found that they were remarkably similar (Fig. 1*G*), indicating that FBLL1 might be a potential 2′-O-methyltransferase located in the brain.

FBLL1 Functionally Catalyzes RNA Nm in Cells. To further investigate whether FBLL1 is a MTase and its methylation function, we overexpressed (OE) *FBLL1* in HEK293T, HeLa, and neuro2a cells and then checked changes in the abundance of Nm. Because FBLL1 is specifically expressed in the brain, we also knocked-down (KD) *FBLL1* in neuro2a cells, a fast-growing neuroblastoma cell line isolated from mouse brain tissue. Meanwhile, the same procedures were conducted for FBL as a control. WB results validated that FBL/FBLL1 was successfully OE or KD at the protein level. A positive correlation was observed between the levels of Nm modification and FBLL1 or FBL expression (Fig. 2 *A*–*D* and *SI Appendix*, Fig. S3), suggesting that FBLL1 does have 2′-O-methyltransferase activity in cells.

FBL is an essential nucleolar protein that is enriched in the dense fibrillar component and participates in pre-rRNA processing by mediating Nm modifications (18). Given that FBLL1 showed similar ability to FBL to catalyze methylation, we hypothesized that FBLL1 is also located in the nucleolus. The subcellular location of FBLL1 was subsequently determined using immunofluorescence (Fig. 2*E*). Myc-tagged FBLL1 and FBL were expressed in A549 cells and visualized, with nucleolin as a nucleolus marker. The merged image indicated that FBLL1 was distributed in the nucleolus, suggesting that FBLL1 might share a similar catalytic mechanism to FBL by forming a box C/D snoRNP complex.

FBLL1 Is a Key Enzyme of a snoRNA-Guided RNP Catalytic Complex. To determine whether FBLL1 catalyzes Nm modification on its own or as part of a protein complex, we conducted coimmunoprecipitation (co-IP) experiments to identify proteins that interact with FBLL1. In eukaryotes, FBL methylates RNA by forming a RNP complex with other core proteins and guide snoRNAs. The catalytic complexes share a common set of four key proteins: FBL, NOP56, NOP58, and NHP2L1 (23). In FBLL1-IP samples, core proteins including NOP56, NOP58, and NHP2L1 were significantly enriched (Fig. 3*A* and *SI Appendix*, Fig. S4*A*). A Pearson correlation of >0.95 was observed for the interactomes of FBLL1 and FBL (*SI Appendix*, Fig. S4*C*), suggesting that their interaction patterns are highly comparable. The interactions between FBLL1 and other core proteins were confirmed by WB following pull-down assays (Fig. 3*B*). All the data indicate that FBLL1 may be required to form a RNP complex to exert its catalytic activity.

We then attempted to reconstitute functional human box C/D RNP complexes by using recombinant proteins. Unfortunately, human NOP56 and NOP58 easily aggregated during purification and we were not able to obtain stable proteins, which was similar to previous studies (27). After analyzing published eukaryotic box C/D snoRNP models from yeast to mammals, we hypothesized that NOP56 and NOP58 from the thermophilic yeast *Chaetomium thermophilum* (Ct) (27) might interact with human FBLL1/FBL to form a core catalytic complex. We first coexpressed Ct-NOP56/Ct-NOP58 with human FBLL1 and obtained stable FBLL1-NOP56/NOP58 complexes. Human NHP2L1 were purified separately and added later for protein assembly into FBLL1–RNP complex. And FBL-RNP was isolated in the same way. All recombinant proteins were confirmed by MS analysis (*SI Appendix*, Fig. S5 *A*–*D*). Electrophoretic mobility shift assays were carried out to detect protein complex–RNA interactions. Compared with free RNAs, protein–RNA complexes migrate more slowly (Fig. 3*C*). The data indicated that the recombinant FBLL1 protein complex interacted with guide snoRNA (U46) in vitro.

The FBLL1–RNP Complex Transfers Methyl Groups to Substrate RNAs In Vitro. To evaluate the ability of reconstituted FBLL1–RNP complex to catalyze methylation, we performed an in vitro assay by incubating it with guide box C/D snoRNA (U46), paired substrate RNA (Am3739), and methyl donor *S*-adenosylmethionine (SAM). After reaction for 4 h at 37 °C, nucleases were added to digest RNA and the resulting products were analyzed by LC–MS (Fig. 3*D*). The preliminary results showed a peak with a retention time (RT) of 6.53 min in the extracted ion chromatogram (XIC, Am M^+ = 282.1202) after in vitro methylation using FBLL1–RNP. No such transfer was detected when denatured proteins were used or SAM was not added. The RT and fragmentation patterns were identical to those of the Am standard, indicating that methyl groups were successfully transferred to the substrate RNA by the FBLL1–RNP complex. (Fig. 3 *E* and *F* and *SI Appendix*, Fig. S6 *A* and *B*).

In the snoRNP, NHP2L1 helps position the guide snoRNA in an active conformation (28). A previous study showed that the Fib–Nop5 (FBL-NOP56/NOP58 in mammals) complex of *Pyrococcus abyssi* (a hyperthermophilic archaeon) could carry out Nm modifications (26). Here, our findings suggest that NHP2L1 is essential for the catalytic activity of the FBLL1–RNP complex (Fig. 3*E*). This necessity may stem from the greater complexity of eukaryotic RNPs compared with their archaeal counterparts, leading to more stringent limitations on the catalytic processes.

Several studies have highlighted the significance of residue D236 in human FBL for the catalytic activity (26, 29). After comparing the sequence and structure of FBLL1 with FBL, we hypothesized that residue D248 in FBLL1, which is located in the SAM-binding pocket, might play a critical role in mediating methylation. Molecular docking results showed that the binding energy between FBLL1 and SAM slightly increased from WT (−6.592 kcal/mol) to D248A (−6.384 kcal/mol). Meanwhile, the results indicated that D248 is close to the reaction center and maybe get involved into the catalysis process as shown in previous studies (24). (Fig. 3 *G* and *H*). We mutated residue D248 of FBLL1 to alanine and found that the interaction between the mutant human FBLL1 and Ct-NOP56/Ct-NOP58 was not affected (*SI Appendix*, Fig. S5 *E* and *F*). However, the catalytic activity reduced to 5% of the wild type when FBLL1 in the RNP complex was replaced with FBLL1 D248A (Fig. 3*I* and *SI Appendix*, Fig. S6*C*). Considering the predicted binding energy from WT to D248A mutant is trivial, the charged aspartate residue may play a critical role in maintaining catalytic activity.

FBLL1 Shows Broad Activity with Box C/D snoRNAs as Guides. Both in cellular and in vitro assays confirmed that FBLL1 could catalyze Nm after protein assembly into a RNP complex with other components. Previous studies have revealed that FBL is

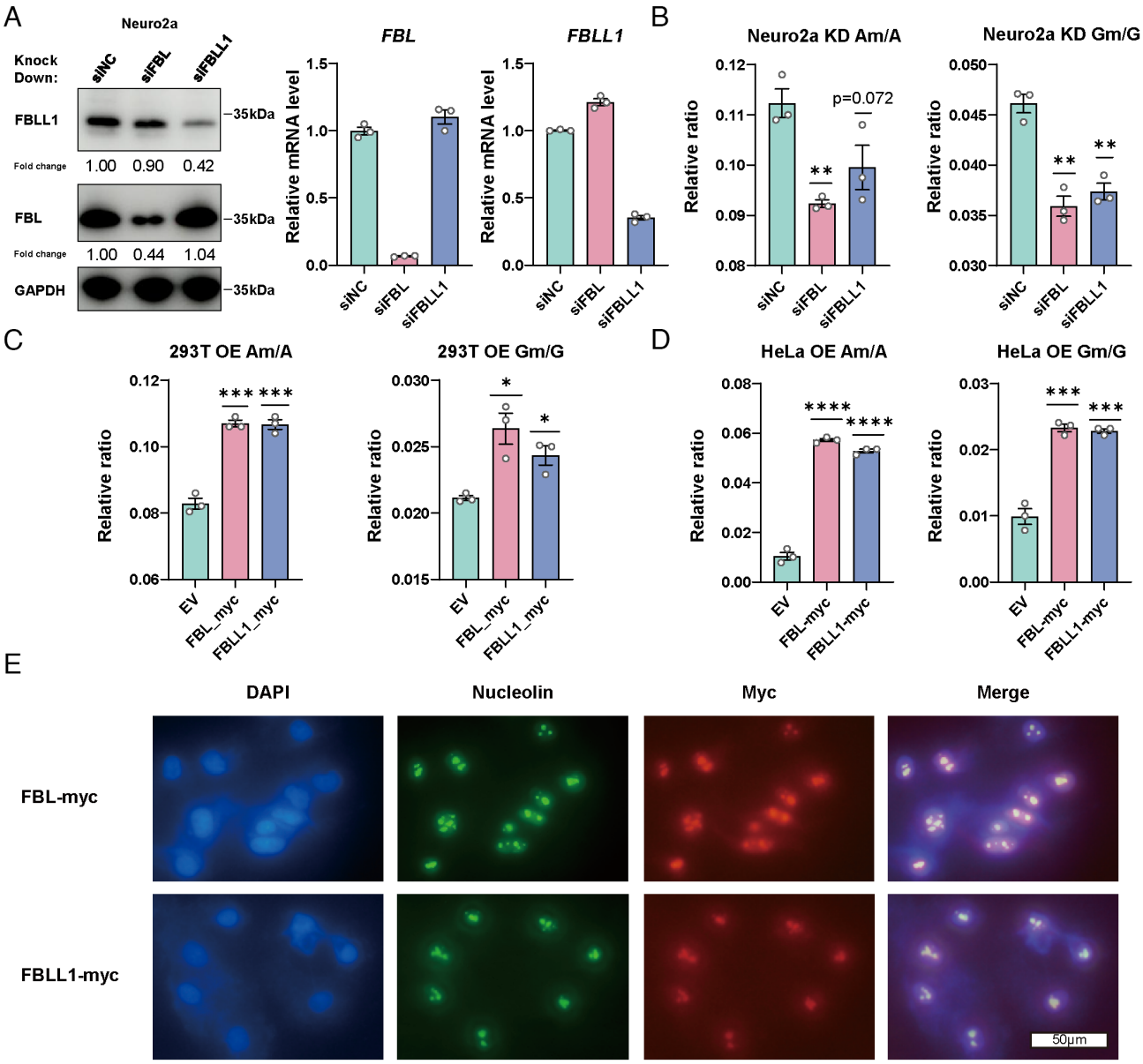

Fig. 2. FBLL1 catalyzes RNA Nm intracellularly. (*A*) WB and RT-qPCR results following transfection of neuro2a cells with FBL or FBLL1 siRNAs. (*B–D*) 2′-O-methylation levels of adenosine (A) and guanosine (G) in total RNAs of neuro2a, 293 T, and Hela cells transfected with siRNA or expression vectors, quantified by LC–MS. (*E*) Immunofluorescence labeling of Myc (red) in A549 cells transfected with FBL-myc or FBLL1-myc expression vectors. The nucleoli (green) were costained using an anti-Nucleolin antibody followed by Alexa-Fluor-conjugated (AF488 and AF594) secondary antibody, and the nuclei were visualized by using DAPI (DAPI, blue). (Scale bars, 50 μm.) Error bars, mean ± SEM; n = 3 (*A–D*) biologically independent samples. **P* < 0.05, ***P* < 0.01, and ****P* < 0.001.

responsible for forming multiple Nm sites in rRNAs using box C/D snoRNAs as guides. To investigate the relevance of FBLL1 in rRNA Nm modifications, we synthesized 14 snoRNAs and their paired substrate RNAs (selected from human 28S, 18S, and 5.8S rRNAs; data from snoDB: https://bioinfo-scottgroup.med.usherbrooke.ca/snoDB/) (30) and performed in vitro methylation experiments. The Am, Gm, Cm, and Um products were successfully characterized by LC–MS, demonstrating that FBLL1 has broad reactivity and can transfer methyl groups to multiples sites of rRNAs (Fig. 4 *A* and *B* and *SI Appendix*, Fig. S7).

FBLL1 Exhibits Different Nm Site Preferences Compared with FBL. We noticed that FBLL1 showed different catalytic efficiencies toward distinct Nm sites (*SI Appendix*, Fig. S7 *A–D*), which is similar to FBL (13). The main reason for the specificity of reactivity on different based could be the differences in binding affinity between different guide snoRNAs and the catalytic protein complex, which are impacted by many factors. Previous studies show that the four key proteins in the FBL catalytic complex (including FBL, NOP56, NOP58, NHP2L1), as well as the sequence of snoRNA, can influence the binding affinity, and contribute to the differences of reactivity toward different bases (27, 31, 32).

To explore the differences between FBLL1 and FBL, we analyzed their in vitro methylation activities and found that they preferentially methylated different substrates (Fig. 4 *C* and *D*). FBLL1 showed its highest activity with U16 compared with U51 and U46. Meanwhile, FBL showed its highest activity with U51, but catalyzed little methylation of Am 484 under the guidance of U16.

We then used RTL-P [Reverse Transcription at Low deoxyribonucleoside triphosphate (dNTP) concentrations followed by PCR] (33) to evaluate the changes of selected Nm sites after knocking-down *FBL* or *FBLL1* in neuro2a cells (Fig. 4*E*).

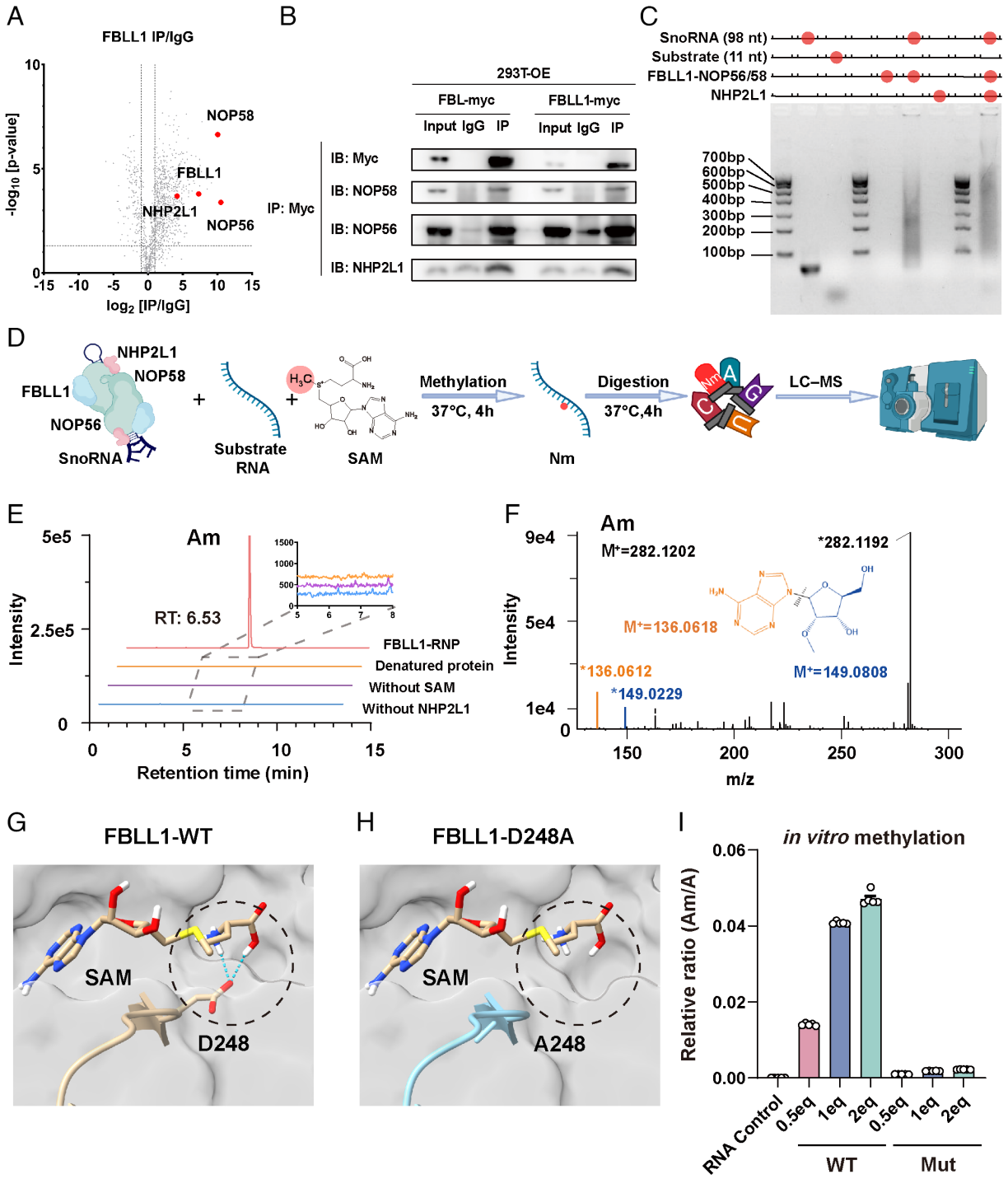

Fig. 3. FBLL1 transfers methyl groups to substrate RNAs in vitro by forming snoRNP complexes. (*A*) Volcano plots of proteomic analysis of co-IP of FBLL1–myc using Myc-antibody in 293 T cells transfected with expression vectors, compared with IgG isotype. (*B*) Co-IP results confirmed FBLL1 interacts with other Box C/D snoRNP complex proteins. (*C*) Binding results of FBLL1–RNP complex and snoRNA measured by the electromobility shift assay. The FBLL1–RNP complex and NHP2L1 interacted with human snoRNA46 (U46). (*D*) General strategy of in vitro methylation and detection of 2′-O-methylation products by LC–MS. (*E*) Extracted ion chromatogram (XIC) of Am 282.1202 ± 0.01 Da. In vitro methylation result of U46 by FBLL1–RNP compared with that by denatured protein or in the absence of *S*-adenosylmethionine (SAM), or in the absence of NHP2L1. Each part of the complex is vital. RT: retention time. (*F*) Tandem mass spectrum of the Am product. Am splits into two ions with *m/z* 136.0612 and 149.0229 by breaking the chemical bond along the dotted line. (*G* and *H*) The molecular docking structure of SAM with wild-type human FBLL1 or mutant human FBLL1 (D248A). Blue dot lines, hydrogen bonds between SAM and FBLL1-WT. (*I*) Catalytic activity of FBLL1 (D248A)–RNP complex in vitro catalytic activity compared with that of wild-type FBLL1–RNP complex proteins by measuring the product Am ratio. Error bars, mean ± SEM; n = 5 independent samples.

Coordinated with in vitro results, the methylation level of Am 485 guided by U16 in mouse were significantly decreased after RNA interference with FBLL1 (siFBLL1) but not siFBL, suggesting that FBLL1 is the predominant 2′-O-methyltransferase of Am 485. Meanwhile, FBL catalyzed methylation of Am 1337 better than FBLL1 in mouse, which was also consistent with in vitro data. The high correlation between cellular site selectivity and in vitro reactivity preferences indicates that FBLL1 and FBL have distinct substrate specificities.

Considering that the most variable region between FBLL1 and FBL is the *N*-terminal G/R-rich domain and MTase domain is highly conserved, we hypothesized that the differences in

A

	18S rRNA				28S rRNA								5.8S rRNA	
Name (snoRNA)	U11	U16	U28	U61	U6	U24	U34	U41	U46	U51	U53	U80	U71	U96A
Position (in human)	Gm509	Am484	Cm1391	Um1442	Gm2411	Cm2338	Um2824	Um4276	Am3739	Am1511	Cm3848	Gm1612	Um14	Gm75
Position (in mouse)		Am485							Am3416	Am1337				

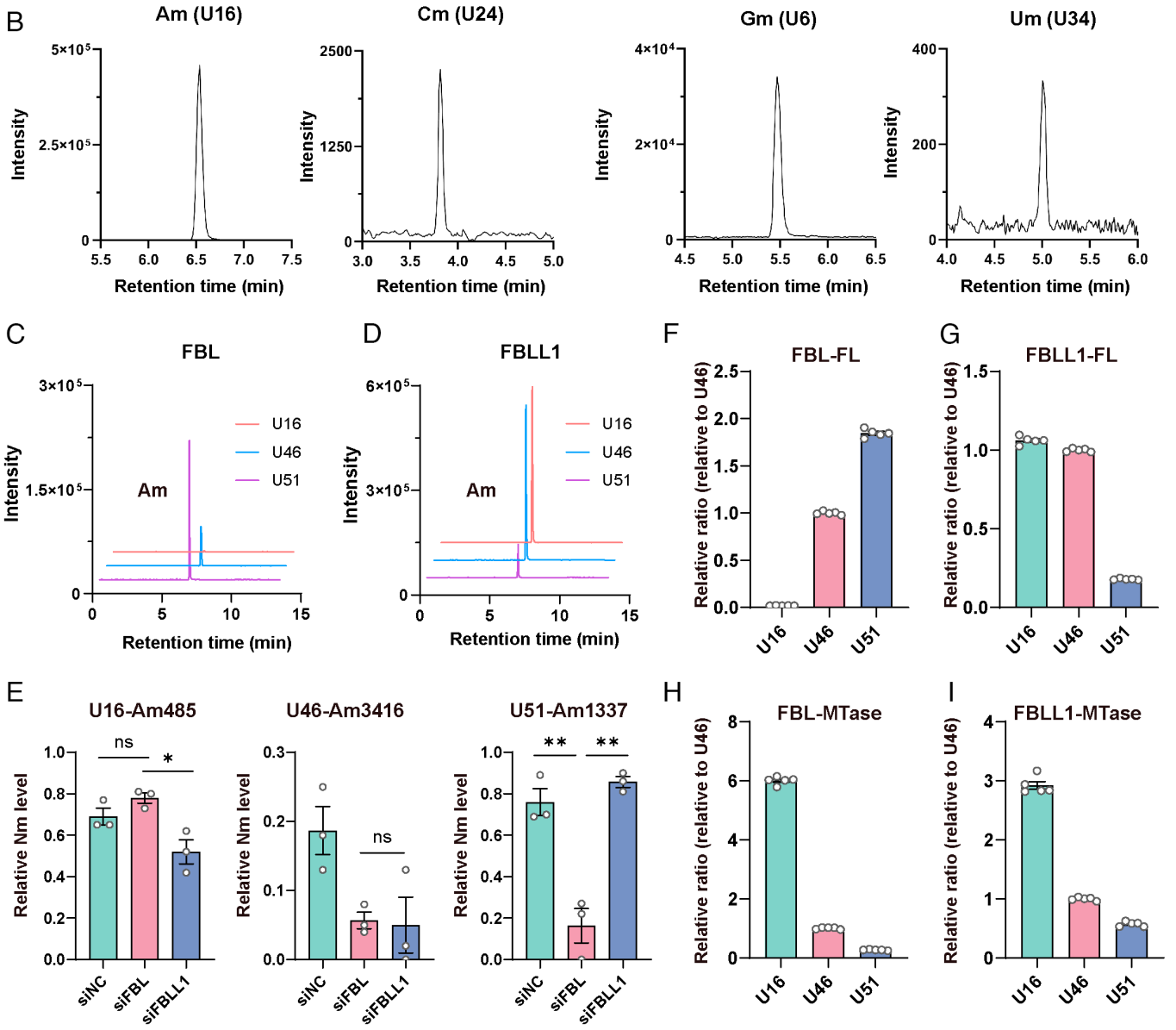

Fig. 4. FBLL1 shows broad reactivity and exhibits site-selective catalytic activity. (*A*) Table of different snoRNAs (from U6 to U96A) and their targets. (*B*) Representative results for in vitro methylation of Am (U16), Gm (U6), Cm (U24), and Um (U34) using FBLL1–RNP complex. (*C*) In vitro methylation of three Am-targeted snoRNAs, U16, U46, and U51, by the FBL–RNP complex shows that FBL prefers U51. (*D*) In vitro methylation of three Am-targeted snoRNAs, U16, U46, and U51, by the FBLL1–RNP complex shows that FBLL1 prefers U16. (*E*) Reverse Transcription at Low deoxyribonucleoside triphosphate (dNTP) concentrations followed by the PCR assay (RTL-P assay) to measure U16, U46, and U51 target 2′-O-methylation levels after knockdown of *FBL* or *FBLL1* in neuro2a cells. (*F–I*) Quantification of catalytic activity of FBL-FL, FBLL1-FL, FBL-MTase, FBLL1-MTase with U16, U46, and U51. Error bars, mean ± SEM; n = 3 (*E*) and n = 5 (*F–I*) independent samples. **P* < 0.05, ***P* < 0.01, and ****P* < 0.001.

reaction preferences could be due to the G/R-rich domain. We then reconstituted box C/D RNP complexes using the MTase domains of FBL or FBLL1 (*SI Appendix*, Fig. S5 *G* and *H*) and checked their reaction selectivity. Unlike RNP complexes with full-length (FL) proteins, the FBLL1-MTase RNP showed similar catalytic patterns with FBL-MTase RNP (Fig. 4 *F–I*). These results indicated that the N-terminal domain of FBLL1 (the noncatalytic domain) contributes to its site selectivity, distinguishing it from FBL functionally.

FBLL1 Is Required for Neuronal Differentiation. Our previous findings indicate that FBLL1 is primarily expressed in the brain (Fig. 1*E*), and it exhibits distinct Nm site preferences compared with FBL (Fig. 4 *C–I*). We next examined the major location of FBLL1 by immunohistochemical (IHC) staining of human brain tissues. Several different subregions were examined, including the middle frontal gyrus (MFG), superior temporal gyrus (STG), cornu ammonis 1-4 (CA1-4), dentate gyrus (DG), and entorhinal cortex (EC). Consistent with data from The Human Protein Atlas

(34), FBLL1 was enriched in human neuron cells in brain tissues (Fig. 5*A* and *SI Appendix*, Fig. S8). We also checked the protein levels of FBLL1 in different regions of mouse brain samples and found it broadly expressed in brain tissues (Fig. 5*B*). We reanalyzed our proteome datasets by comparing FBLL1-IP with FBL-IP results (Datasets S1 and S2). Gene Ontology analysis using Metascape (35) revealed that proteins significantly more abundant in FBLL1-IP samples were associated with nervous system development (Fig. 5*C* and *SI Appendix*, Fig. S4*B*). Meanwhile, we noticed that *FBLL1* is specifically enriched in cluster 22 whose main function is synaptic signal transduction in the brain (data from The Human Protein Atlas).

Neuro2a cells are an extensively used model system to study neuronal differentiation, axonal growth, and signaling pathways (36). Here, we used all-*trans* retinoic acid (ATRA) to induce neural differentiation and axon outgrowth in neuro2a cells (Fig. 5*D*). Following ATRA treatment, cells displayed an augmentation in both number of neurites and neurite length, which were repressed by siFBLL1. Conversely, siFBL did not yield a significant difference in the observed results (Fig. 5*E*). These data demonstrate a unique role of FBLL1 in neuronal differentiation.

We next wondered whether FBLL1 promotes neuronal differentiation through regulation of synaptic growth. GAP43, also known as neuromodulin, is a vital protein involved in axonal growth, contributing to extracellular growth and nerve cell regeneration (37). Through correlation analysis using GoPIA in Gene Expression Profiling Interactive Analysis (38), we found a linear relationship between the expression levels of *GAP43* and *FBLL1* in normal human brain samples, but not between *GAP43* and *FBL* (Fig. 5*F*). Subsequent RT-qPCR results validated that knocking-down *FBLL1*, but not *FBL*, led to a significant decrease in *GAP43* mRNA levels upon ATRA stimulation, consistent with outcomes at the protein level (Fig. 5 *G* and *H*). Moreover, the expression level of GAP43 protein was increased in FBLL1-OE cells even without ATRA treatment (*SI Appendix*, Fig. S9*A*). All the data suggest that FBLL1 is required for neuronal differentiation and plays a distinct role from FBL.

FBLL1 Promotes Neuronal Differentiation through Nm Modifications of *GAP43* mRNA to Enhance Its Protein Expression. We then asked how FBLL1 mediates neuronal differentiation via GAP43. Previous studies have shown that internal Nm modifications of mRNA can be guided by snoRNAs and influence mRNA and protein expression (39, 40). Given that our data show that FBLL1 catalyzes RNA Nm in a Box C/D snoRNA-dependent way, we speculated that FBLL1 may mediate the Nm modifications in *GAP43* mRNA and hence regulate GAP43 protein expression.

Given that no Nm modification sites have been reported in published studies (41), we used RTL-P to anchor FBLL1-mediated Nm sites in *GAP43* mRNA CoDing Sequence region with three primers: Primer-H (head), Primer-M (middle), and Primer-T (tail) for detection of longer, mid-length, and shorter cDNA products, respectively (Fig. 6*A*). Compared with control, products of Primer-H were significantly reduced after FBLL1-OE, where no changes were observed with Primer-T and slight decrease with Prime-M, suggesting that there might be multiple FBLL1-mediated Nm sites in *GAP43* mRNA between region of 182-619 (Fig. 6*B*).

To investigate the precise regulatory mechanisms of FBLL1 in neuronal differentiation, we detected Nm changes in *GAP43* mRNA after knocking-down FBLL1 (Fig. 6*C*). No changes were observed between products of different primers after FBLL1-KD when ATRA was absent, and the expression of GAP43 protein was neither affected (Fig. 5*G*). Once ATRA was added, products of Primer-H were significantly increased after FBLL1-KD, leading to a decreased expression of GAP43 protein. It could be because Nm sites in *GAP43* were blocked by siFBLL1, which were expected to be up-regulated upon ATRA stimulation. Meanwhile, no such changes in *GAP43* Nm modification or GAP43 protein levels were detected after knocking-down FBL, further indicating a distinct role of FBLL1 from FBL.

For the mechanistic insight into how Nm controls the expression of GAP43, we measured the GAP43 mRNA stability using transcription inhibition by Actinomycin D (ActD) as several studies showed that the internal Nm of mRNA regulated its stability (16, 32). Accelerated mRNA decay of GAP43 was confirmed when knocking down FBLL1 but not FBL in Neuro2a cells (Fig. 6*D* and *SI Appendix*, Fig. S9*B*), indicating an unstable status of GAP43 mRNA because of the reduced Nm levels upon loss of FBLL1. We also measured the ribosome binding ability of GAP43 mRNA by the Polysome assay. The relative ratio of actively translated mRNA was not changed (*SI Appendix*, Fig. S9 *C–E*), suggesting that the translation activity of GAP43 mRNA was not affected by siFBLL1. However, the total amount of ribosome-binding GAP43 mRNA was significantly decreased when knocking down FBLL1 (Fig. 6*E*), which is consistent with the decreased GAP43 mRNA stability under siFBLL1.

To further investigate how FBLL1 affected the protein expression level of GAP43, we then checked the freshly produced GAP43 during neuron differentiation by SUnSET (42). We labeled newly processed protein with puromycin and measured GAP43 using its specific antibody after pull-down. Results showed the amount of newly produced GAP43 decreased significantly when FBLL1 was knocked down and siFBL did not affect GAP43 protein synthesis (Fig. 6*F* and *SI Appendix*, Fig. S9*F*). Our results show that FBLL1 regulates the GAP43 protein expression by influencing the GAP43 mRNA stability through mediating its Nm modifications.

Altogether, the strong correlation between *GAP43* mRNA Nm modifications, GAP43 protein level, and FBLL1 indicates that FBLL1-mediated Nm modifications of *GAP43* mRNA enhance the protein expression of GAP43, which consequently promotes neuronal differentiation (Fig. 6*G*).

Discussion

Increasing numbers of studies have revealed that dysregulation of Nm modifications causes various diseases, including cancer, neurodegeneration, and autoimmune diseases (20, 43, 44). The regulatory mechanisms are generally elucidated from expression changes of the Nm writer proteins because no erasers or readers have been identified. Meanwhile, most of the reported research focuses on the only previously known snoRNP 2′-O-methyltransferase FBL, because it can transfer methyl groups to rRNA, mRNA, and other types of RNA. For example, we previously revealed that decreased Nm modifications induced by FBL-KD in macrophages promote an innate immune response (20). Here, we identified FBLL1 as a Nm transferase. Like FBL, it shows snoRNP-dependent catalytic activity and is able to introduce methyl groups onto a broad range of rRNA and mRNA. It is unclear whether FBLL1 participates in the FBL-related regulatory pathways; how the two enzymes coordinate, in competition or cooperation, is worthy of further study.

FBLL1 is preferentially located in the brain and exhibits distinct Nm site preferences compared with FBL. The differences in tissue distribution and reaction selectivity between FBL and FBLL1 could be due to the sequence variation of the *N*-terminal G/R-rich domain. Our results suggest that FBLL1 may have a similar expression level to FBL in mouse brain tissue (Fig. 1*C*). Current commercially available antibodies against FBL (e.g., from CST and Abcam)

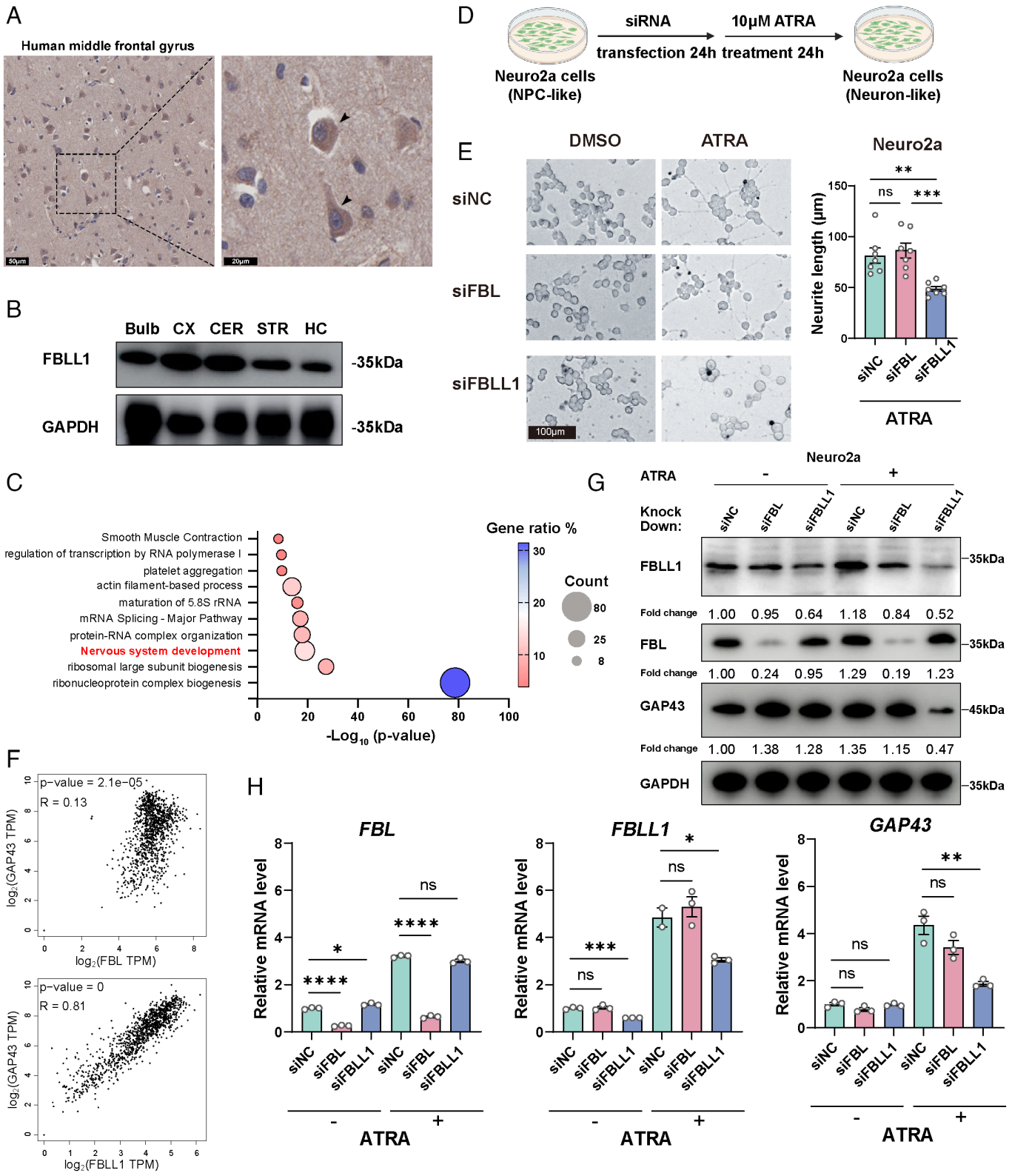

Fig. 5. FBLL1 is required for neuronal differentiation. (*A*) Immunohistochemistry of human MFG using anti-human FBLL1 antibody indicates FBLL1 locates in neurons. [Scale bars, 50 μm (*Left*), 20 μm (*Right*).] (Sample from the human brain No. 2.) (*B*) WB analysis of FBLL1 protein level in five different parts of the mouse brain (Olfactory bulb, Bulb; cerebral cortex, CX; Cerebellum, CER; Striatum, STR; Hippocampus, HC). (*C*) Gene Ontology-based functional classification of different proteins that were up-regulated in the FBLL1–myc IP group compared with FBL–myc IP group. The data were obtained from three independent biological replicates. (*D*) Model of the Neuro2a cell differentiation assay. (*E*) Representative images of neuro2a cell knockdown negative controls, or with knockdown of FBL or FBLL1, treated with 10 μM all-*trans* retinoic acid (ATRA) or dimethylsulfoxide (DMSO) for 48 h. In FBLL1-knockdown neuro2a cells, neurite lengths (randomly selected, shown in *SI Appendix*, Fig. S9 *A*–*C*) are shorter than those in FBL-knockdown or negative control cells. (*F*) Correlation analysis of *FBL* or *FBLL1* with *GAP43* by Gene Expression Profiling Interactive Analysis, using Genotype-Tissue Expression Portal (GTEx) data for the brain. (*G*) FBL, FBLL1, and GAP43 protein levels in neuro2a cells measured by WB. (*H*) *FBL*, *FBLL1*, and *GAP43* mRNA levels in neuro2a cells measured by RT-qPCR. Error bars, mean ± SEM; n = 7 (*E*) and n = 3 (*H*) independent samples. **P* < 0.05, ***P* < 0.01, ****P* < 0.001 and *****P* < 0.0001.

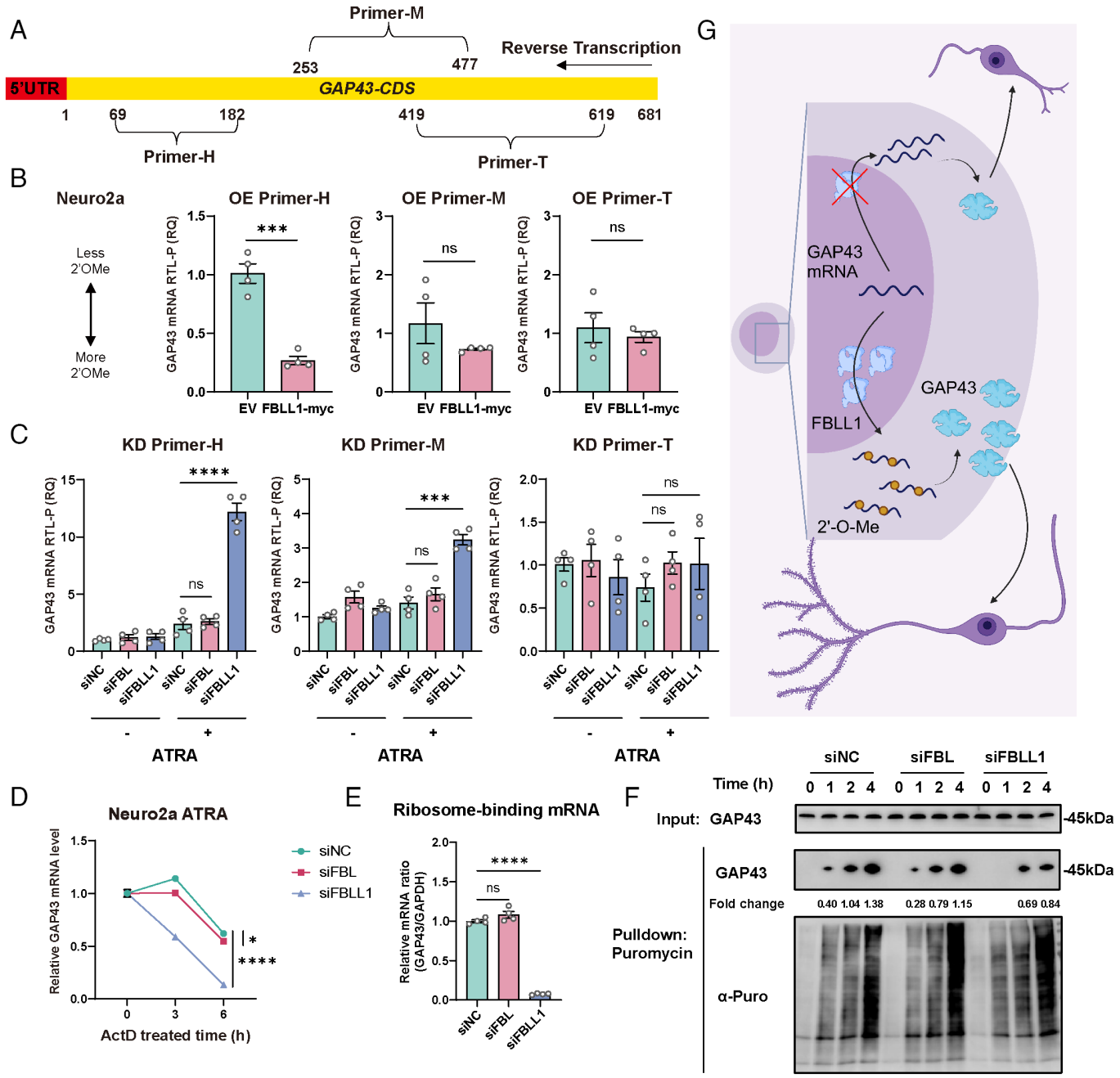

Fig. 6. FBLL1 promotes neuron differentiation through *GAP43* mRNA Nm modification. (*A*) Primers used to measure *GAP43* mRNA Nm level by using RTL-P. (*B* and *C*) RTL-P results measuring *GAP43* mRNA internal 2′-O-methylation levels in overexpression or KD neuro2a cells. A lower methylation level results in more transcripts products. (*D*) GAP43 mRNA stability test in neuro2a cells treated with ActD. (*E*) Ribosome-binding GAP43 mRNA measured by RT-qPCR. (*F*) Newly processed GAP43 was measured by the SUnSET assay. (*G*) Model of FBLL1 regulating *GAP43* mRNA internal 2′-O-methylation levels, which promotes neuron differentiation. [Figure created with Biorender.com] Error bars, mean ± SEM; n = 4 (*B*–*E*) independent samples. **P* < 0.05, ***P* < 0.01, and ****P* < 0.001.

show cross-reactivity to FBLL1 because they are designed based on the conserved MTase domain. Considering the unique functions of FBLL1 in neuronal differentiation identified in the present study, antibodies with high specificity need to be developed and carefully evaluated to help characterization of the exact biological roles of FBL and FBLL1, especially in neurons or brain samples.

Translational control plays a crucial role in regulating gene expression in various cellular processes. Numerous studies have highlighted the emergence of dynamic mRNA modifications as a novel regulatory mechanism of translation. For instance, m6A within mRNA coding regions facilitates translation through its interaction with the m6A reader YTHDC2 (45). Recent studies have discovered that mRNA translation can be altered by Nm modifications of mRNA guided by snoRNA, demonstrating the diversity of biological roles of Nm. The regulatory mechanisms are complicated. Some studies have found that Nm disrupts key steps in codon reading during cognate tRNA selection, leading to decreased translation (15, 39). On the contrary, several groups have reported that Nm in mRNA could promote pre-mRNA processing and enhance translation (40, 43). Here, we found that GAP43 was more highly expressed when its mRNA contained a higher number of Nm modifications. KD of *FBLL1* led to decreased Nm levels in *GAP43* mRNA and decreased translation, which eventually repressed axon elongation. This could be explained by the improved stability from Nm modifications of mRNA, but the precise mechanism needs to be investigated.

In summary, we uncover FBLL1 as a snoRNP 2′-O-methyltransferase which is specifically expressed in the brain, especially in human neuron cells. Our data demonstrate that FBLL1 has distinct functions from the previously known FBL, and is required for neuronal differentiation through the regulation of Nm modification of *GAP43* mRNA. The identification of FBLL1 provides insights into the roles of RNA modifications in regulating neuronal differentiation and may contribute to potential therapeutic strategies for Nm-associated human diseases.

Materials and Methods

Mice and Cell Culture. C57BL/6J (6 to 8 wk of age) mice were obtained from Charles River Experimental Animal Company (Beijing, China). All animal experiments conducted in this study were carried out following the guidelines established by the Institutional Animal Care and Use Committee. The study was approved by the Ethics Committee of Nankai University (2023-SYDWLL-000154). HEK293T (293T), HeLa, and A549 cells were obtained from American Type Culture Collection (CRL-3216, CCL-2, and CCL-185). Neuro2a cells (CL-0168) were from Procell Life Science&Technology Co., Ltd. All cells were cultured at 37 °C with 5% CO_2. HEK293T cells were cultured in Dulbecco's modified Eagle's medium (10-013-CV, Corning) supplemented with 10% Fetal Bovine Serum (FBS, 10099-141C, Gibco); HeLa and A549 cells were cultured in RPMI 1640 (10-040-CV, Corning) supplemented with 10% FBS; Neuro2a cells were cultured in Minimum Essential Medium (10-009-CV, Corning) supplemented with 10% FBS, 1% GlutaMax (35050061, Gibco), 1% penicillin–streptomycin (15140122, Gibco).

Human Samples. Paraffin-embedded sections from postmortem human brain tissues were obtained from the National Human Brain Bank for Development and Function, affiliated with the Chinese Academy of Medical Sciences and Peking Union Medical College, situated in Beijing, China. Individuals with neurodegenerative disease (Alzheimer's disease, Parkinson's disease, etc) or cerebrovascular disease (Stroke, intracranial hemorrhage, et al) were not included. Four postmortem brains (three males and one female, 75.0 ± 16.8 y) with seven subregions, including MFG, STG, CA1, CA2, CA3, CA4/DG, and EC, were used for IHC staining (MFG; STG; CA1-4; DG; EC).

The human brain tissues were fixed with 4% paraformaldehyde, followed by gradient dehydration in alcohol and xylene, and then embedded in paraffin. All processes involving human tissues adhered to the Standardized Operational Protocol for Human Brain Banking in China (46). This study was approved by the Ethics Committee of the Institute of Basic Medical Sciences Chinese Academy of Medical Sciences (Approval Number: 009-2014).

Other Methods. RNAi and plasmids, cell differentiation, RNA purification and RT-qPCR, Immunofluorescence staining, MS analysis of RNA modifications, Western blotting, Immunoprecipitation, Polysome assay, Metabolic labeling, MS analysis of proteins, Protein expression and purification, Molecular docking, In vitro methylation assay, Reverse Transcription at Low dNTP concentrations followed by PCR (RTL-P), Immunohistochemistry, and RNA stability assay for mRNA lifetime assay can be found in Supplementary Materials and Methods (*SI Appendix*).

Quantification and Statistical Analysis. The statistical significance of comparisons between two groups was analyzed with Student's *t* test. Differences were considered to be statistically significant when *P* values were less than 0.05.

Data, Materials, and Software Availability. All study data are included in the article and/or supporting information.

ACKNOWLEDGMENTS. We thank Dr. Keqiong Ye for kindly providing Ct-NOP56 and Ct-NOP58 vectors. We thank the MS Platform of the College of Life Sciences, Nankai University, for supporting our work. This research was supported by grants from the National Natural Science Foundation of China (82388201 and 32370960), the CAMS (Chinese Academy of Medical Sciences) Innovation Fund for Medical Sciences (2021-I2M-1-017), and the State Key Laboratory of Medicinal Chemical Biology of Nankai University (BB042411, 9242000502, and ZB231012).

1. M. Frye, B. T. Harada, M. Behm, C. He, RNA modifications modulate gene expression during development. *Science* **361**, 1346–1349 (2018).
2. I. Barbieri, T. Kouzarides, Role of RNA modifications in cancer. *Nat. Rev. Cancer* **20**, 303–322 (2020).
3. D. Han, M. M. Xu, RNA modification in the immune system. *Annu. Rev. Immunol.* **41**, 73–98 (2023).
4. J. e. Liu *et al.*, Landscape and regulation of m6A and m6Am methylome across human and mouse tissues. *Mol. Cell* **77**, 426–440.e6 (2020).
5. J. Liu, X. Cao, RBP–RNA interactions in the control of autoimmunity and autoinflammation. *Cell Res.* **33**, 97–115 (2023).
6. H. Ma *et al.*, N6-Methyladenosine methyltransferase ZCCHC4 mediates ribosomal RNA methylation. *Nat. Chem. Biol.* **15**, 88–94 (2018).
7. S. J. Häfner *et al.*, Ribosomal RNA 2′-O-methylation dynamics impact cell fate decisions. *Dev. Cell* **58**, 1593–1609.e9 (2023).
8. M. E. Hess *et al.*, The fat mass and obesity associated gene (Fto) regulates activity of the dopaminergic midbrain circuitry. *Nat. Neurosci.* **16**, 1042–1048 (2013).
9. K. D. Meyer *et al.*, Comprehensive analysis of mRNA Methylation reveals enrichment in 3′ UTRs and near stop codons. *Cell* **149**, 1635–1646 (2012).
10. Y. Liu *et al.*, N6-methyladenosine RNA modification–mediated cellular metabolism rewiring inhibits viral replication. *Science* **365**, 1171–1176 (2019).
11. K. W. Seo, R. E. Kleiner, Profiling dynamic RNA–protein interactions using small-molecule-induced RNA editing. *Nat. Chem. Biol.* **19**, 1361–1371 (2023).
12. J. Song, Y. Zhuang, C. Yi, Programmable RNA base editing via targeted modifications. *Nat. Chem. Biol.* **20**, 277–290 (2024).
13. J. Erales *et al.*, Evidence for rRNA 2′-O-methylation plasticity: Control of intrinsic translational capabilities of human ribosomes. *Proc. Natl. Acad. Sci. U.S.A.* **114**, 12934–12939 (2017).
14. D. Li *et al.*, Activity dependent LoNA regulates translation by coordinating rRNA transcription and methylation. *Nat. Commun.* **9**, 1726 (2018).
15. B. A. Elliott *et al.*, Modification of messenger RNA by 2′-O-methylation regulates gene expression in vivo. *Nat. Commun.* **10**, 3401 (2019).
16. L. Chen *et al.*, Nm-Mut-seq: A base-resolution quantitative method for mapping transcriptome-wide 2′-O-methylation. *Cell Res.* **33**, 727–730 (2023).
17. M. Zhang *et al.*, A snoRNA-tRNA modification network governs codon-biased cellular states. *Proc. Natl. Acad. Sci. U.S.A.* **120**, e2312126120 (2023).
18. P. V. Sergiev, N. A. Aleksashin, A. A. Chugunova, Y. S. Polikanov, O. A. Dontsova, Structural and evolutionary insights into ribosomal RNA methylation. *Nat. Chem. Biol.* **14**, 226–235 (2018).
19. J. N. Yelland, J. P. K. Bravo, J. J. Black, D. W. Taylor, A. W. Johnson, A single 2′-O-methylation of ribosomal RNA gates assembly of a functional ribosome. *Nat. Struct. Mol. Biol.* **30**, 91–98 (2022).
20. P. Li *et al.*, RNA 2′-O-methyltransferase fibrillarin facilitates virus entry into macrophages through inhibiting type I interferon response. *Front. Immunol.* **13**, 793582 (2022).
21. G. Zheng *et al.*, ALKBH5 is a mammalian RNA demethylase that impacts RNA metabolism and mouse fertility. *Mol. Cell* **49**, 18–29 (2013).
22. F. Liu *et al.*, ALKBH1-mediated tRNA demethylation regulates translation. *Cell* **167**, 816–828.e16 (2016).
23. U. Rodriguez-Corona, M. Sobol, L. C. Rodriguez-Zapata, P. Hozak, E. Castano, Fibrillarin from Archaea to human. *Biol. Cell* **107**, 159–174 (2015).
24. J. Lin *et al.*, Structural basis for site-specific ribose methylation by box C/D RNA protein complexes. *Nature* **469**, 559–563 (2011).
25. M. Ringeard, V. Marchand, E. Decroly, Y. Motorin, Y. Bennasser, FTSJ3 is an RNA 2′-O-methyltransferase recruited by HIV to avoid innate immune sensing. *Nature* **565**, 500–504 (2019).
26. M. Tomkuvienė *et al.*, Archaeal fibrillarin–Nop5 heterodimer 2′-O-methylates RNA independently of the C/D guide RNP particle. *RNA* **23**, 1329–1337 (2017).
27. K. Ye, D. M. J. Lilley, L. Huang, J. Wang, Z. Yang, Functional organization of box C/D RNA-guided RNA methyltransferase. *Nucleic Acids Res.* **48**, 5094–5105 (2020).
28. S. Biswas *et al.*, Comparative analysis of the 15.5kD Box C/D snoRNP core protein in the primitive eukaryote giardia lamblia reveals unique structural and functional features. *Biochemistry* **50**, 2907–2918 (2011).
29. Y. Shi *et al.*, Discovery of cofactor competitive inhibitors against the human methyltransferase fibrillarin. *Pharmaceuticals* **15**, 26 (2021).
30. D. Bergeron *et al.*, snoDB 2.0: An enhanced interactive database, specializing in human snoRNAs. *Nucleic Acids Res.* **51**, D291–D296 (2023).
31. A. Graziadei, F. Gabel, J. Kirkpatrick, T. Carlomagno, The guide sRNA sequence determines the activity level of box C/D RNPs. *Elife* **9**, e50027 (2020).
32. Y. Li *et al.*, 2′-O-methylation at internal sites on mRNA promotes mRNA stability. *Mol. Cell* **84**, 2320–2336.e6 (2024).
33. Z.-W. Dong *et al.*, RTL-P: A sensitive approach for detecting sites of 2′-O-methylation in RNA molecules. *Nucleic Acids Res.* **40**, e157–e157 (2012).
34. M. Uhlén *et al.*, Tissue-based map of the human proteome. *Science* **347**, 1260419 (2015).
35. Y. Zhou *et al.*, Metascape provides a biologist-oriented resource for the analysis of systems-level datasets. *Nat. Commun.* **10**, 1523 (2019).
36. A. Ma'ayan, S. L. Jenkins, A. Barash, R. Iyengar, Neuro2A differentiation by Gαi/o pathway. *Sci. Signal.* **2**, cm1 (2009).
37. S. M. Strittmatter, C. Fankhauser, P. L. Huang, H. Mashimo, M. C. Fishman, Neuronal pathfinding is abnormal in mice lacking the neuronal growth cone protein GAP-43. *Cell* **80**, 445–452 (1995).
38. Z. Tang *et al.*, GEPIA: A web server for cancer and normal gene expression profiling and interactive analyses. *Nucleic Acids Res.* **45**, W98–W102 (2017).
39. J. Choi *et al.*, 2′-O-methylation in mRNA disrupts tRNA decoding during translation elongation. *Nat. Struct. Mol. Biol.* **25**, 208–216 (2018).
40. E. van Ingen *et al.*, C/D box snoRNA SNORD113-6/AF357425 plays a dual role in integrin signalling and arterial fibroblast function via pre-mRNA processing and 2′O-ribose methylation. *Hum. Mol. Genet.* **31**, 1051–1066 (2022).

41. L. Fang *et al.*, Pervasive transcriptome interactions of protein-targeted drugs. *Nat. Chem.* **15**, 1374–1383 (2023).
42. E. K. Schmidt, G. Clavarino, M. Ceppi, P. Pierre, SUnSET, a nonradioactive method to monitor protein synthesis. *Nat. Methods* **6**, 275–277 (2009).
43. B. Lu *et al.*, C/D box small nucleolar RNA SNORD104 promotes endometrial cancer by regulating the 2′-O-methylation of PARP1. *J. Translational Med.* **20**, 618 (2022).
44. M. Abe *et al.*, Impact of age-associated increase in 2′-O-methylation of miRNAs on aging and neurodegeneration in Drosophila. *Genes. Dev.* **28**, 44–57 (2014).
45. Y. Mao *et al.*, m6A in mRNA coding regions promotes translation via the RNA helicase-containing YTHDC2. *Nat. Commun.* **10**, 5332 (2019).
46. W. Qiu *et al.*, Standardized operational protocol for human brain banking in China. *Neurosci. Bull.* **35**, 270–276 (2018).